Anisotropic properties of ultrafast laser-driven microexplosions in lithium niobate crystal

Guangyong Zhou and Min Gu[a)]

center for Micro-Photonics and center for Ultrahigh-bandwidth Devices for Optical Systems (CUDOS),
Faculty of Engineering and Industrial Sciences, Swinburne University of Technology,
PO Box 218, Hawthorn, Victoria 3122, Australia

Smooth voids are achieved in an anisotropic $Fe:LiNbO_3$ crystal with a high refractive index by use of a femtosecond laser-driven microexplosion method. Due to the anisotropy of the crystal, the maximum fabrication depth and the fabrication power threshold are different in different crystal directions, indicating that the direction perpendicular to the crystal axis is more suitable for thick three-dimensional structure fabrication. The dependence of the threshold power on the illumination wavelength shows that the microexplosion mechanism is caused by a two-photon absorption process. As a result, a near threshold fabrication method can be used to generate quasispherical voids. © *2005 American Institute of Physics.* [DOI: 10.1063/1.2142083]

Ultrafast laser-induced breakdown in transparent solid materials has been studied extensively and has received increased attention with the development of high-power femtosecond laser systems.[1–4] By tightly focusing a femtosecond laser beam into transparent materials, multiphoton absorption produces highly localized plasma. The rapid expansion of the plasma causes a microexplosion. In this process, material is ejected from the center, forming a void surrounded by a region of compacted material.[5,6] Void dots or void channels have been generated in a variety of materials from polymers,[6–11] fused silica,[6,12] optical glass to some crystals like quartz and sapphire.[6,8] This method has been used in three-dimensional (3D) optical data storage[4,7] and photonic crystal (PhC) fabrication.[8–14] However, all of the work is concentrated on the isotropic materials with low refractive index such as polymers and glasses. No one, to the best of our knowledge, has applied this optical microfabrication method to anisotropic material with a high refractive index (>2) that is important for PhCs to open a complete band gap.

Lithium niobate ($LiNbO_3$) crystal is a well-known anisotropic nonlinear crystal with a high refractive index of 2.2 and a transparent range of $0.45–5$ μm, which makes it a suitable candidate for near-infrared PhC fabrication. The large nonlinear coefficient of this crystal may result in some nonlinear effects in the PhCs.[15,16] In this letter we report on the generation and characterization of the voids in the Y and Z directions of a Y-cut $LiNbO_3$ crystal. Micron-sized voids have been generated in this crystal by tightly focusing irradiation from a femtosecond oscillator without using an amplifier. Due to the anisotropy of the crystal, the fabrication conditions in different crystal directions have been studied.

The materials used in this work was a Y-cut 0.01% iron-doped $LiNbO_3$ crystal in which the crystal axis is along the Z direction, as shown in Fig. 1(a). The addition of iron ion can reduce the microexplosion threshold by approximately 20% without damaging other properties, so that the fabrication depth can be increased. The crystal was cut into $4\times4\times10$ mm^3 pieces with four large faces (perpendicular to the

Y and Z directions, respectively) polished. The experimental setup was the same as that described elsewhere[9] except that an infrared-enhanced Olympus $60\times$, numerical aperture (NA) 1.4 oil immersion objective and a femtosecond irradiation with a repetition rate of 80 MHz and a pulse width of approximately 50 fs from a Tsunami femtosecond oscillator (Spectra-Physics, USA) were used in the present work. The laser irradiation was focused directly into the sample without a cover slip. The polarization direction of the laser beam is parallel to the Z and Y axis for the fabrication along the Y and Z directions, respectively, as indicated in Fig. 1(a). Low group velocity dispersion mirrors were used to maintain the short pulse. Fabricated voids were characterized by use of a confocal microscope (Fluoview, Olympus, Japan).

Figure 1(b) shows the confocal transmission image of a void at a depth of 5 μm fabricated with a laser power of 500 mW and an exposure time of 10 ms in the Y direction. The transverse diameter of the void is approximately 2 μm. Figure 1(c) shows a depth scanning confocal reflection image of the same void. Two strong reflection signals correspond to the upper and lower surfaces of the void, respectively, indicating the large refractive index contrast and verifying the formation of the void.[7] To further confirm the existence of voids, we polished the crystal to the center of
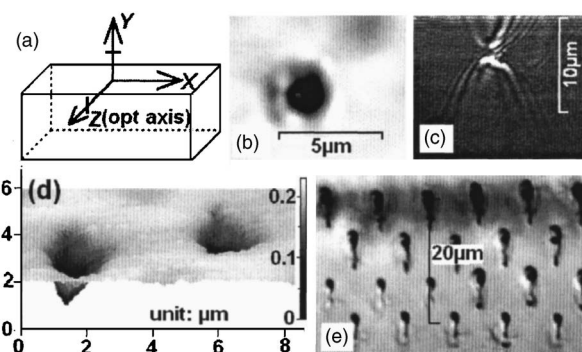
FIG. 1. (a) Sketch of the directions of the $LiNbO_3$ sample and laser polarization. The bars on the Y and Z axis indicate the polarization of the laser beam; (b) and (c) are the confocal transmission image and the depth scanning confocal reflection image of a single void dot, respectively; (d) is the AFM image of the voids; (e) is the sideview confocal transmission image of void dots fabricated at various depths with the same power.

[a)]Author to whom correspondence should be addressed; electronic mail: mgu@swin.edu.au
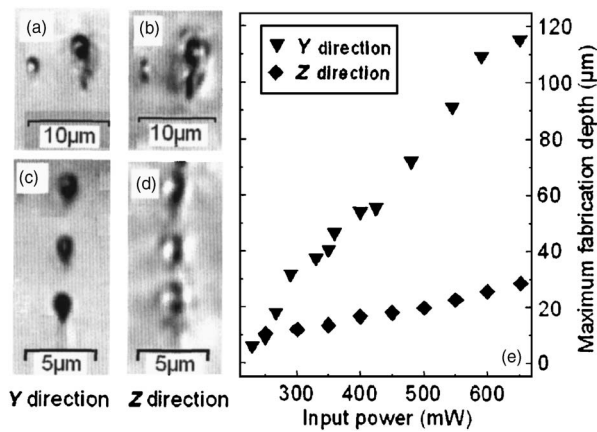
FIG. 2. (a), (c) Comparison of voids fabricated near threshold (left void) and far beyond threshold (right void) for the Y and Z directions, respectively; (b), (d) transmission image of void dots at different depths fabricated near threshold in the Y and Z directions, respectively; (e) maximum fabrication depths as a function of input power in the Y and Z directions.

FIG. 3. (a), (b) Confocal transmission images of voids fabricated with different input powers in the Y and Z directions, respectively; (c) transverse diameters of the voids as a function of the input power in the Y and Z directions; (d), (e) transmission images of voids fabricated with different exposure times in the Y and Z directions, respectively.

the voids and carried out atomic force microscope (AFM) measurement. The AFM image in Fig. 1(d) directly shows the existence of the voids.

To study the axial dimension of the void dots, the sample was rotated by 90° around the X axis after fabrication. Figure 1(d) shows the axial dimension of the void dots fabricated at various depths. The power and the exposure time were fixed at 500 mW and 10 ms, respectively. It can be seen that each dot has a small tail, just like a tadpole. The nonspherical void dots indicate strong distortion of the focal point inside the sample. The reason is a strong spherical aberration effect which is caused by the large refractive index mismatch (~ 0.7) between the crystal (2.2) and the immersion oil (1.52).[17,18] Due to the spherical aberration, the peak intensity at the focal region decreases at a larger depth, and therefore the size of the void decreases.

To produce a 3D array of voids, for example, a photonic band gap structure, one must find a way to generate uniform voids at different depths. By choosing the laser power slightly above the threshold, we have fabricated quasispherical voids. Figure 2(a) shows the axial dimension of two voids dots fabricated with different power levels at a depth of approximately 40 μm in the Y direction. The left void was fabricated with a power of 380 mW that is slightly above the threshold of 350 mW at this depth, while the right void was fabricated with a power of 500 mW. In can be seen that the left side dot is much smaller and much spherical. This result indicates that one can fabricate small quasispherical void dots at different depths by carefully choosing the laser light power. To demonstrate this concept, we fabricated some voids at different depths by choosing the power approximately 30 mW above the threshold, as shown in Fig. 2(c). Although there is still a slightly elongation in the fabrication direction, the voids are much spherical and uniform than those in Fig. 1(d). Similar phenomena were also observed in the Z direction, as shown in Figs. 2(b) and 2(d). For PhCs, the consistency between the voids would be crucial and therefore the laser power must be controlled more accurately.

Due to the refractive index mismatch induced spherical aberration,[17,18] the peak intensity at the focal region decreases when the laser beam is focused deeper. Thus, to get quasispherical voids at a larger depth, one has to increase the power of the input laser light. Figure 2(e) shows the maxi-

mum fabrication depth as a function of the input laser power in the Y and Z directions. One can see that, for a given power, the maximum fabrication depth in the Y direction is much larger than that in the Z direction. For example, at a power of 650 mW, the maximum fabrication depth in the Y direction is 115.5 μm, while that in the Z direction is only 28.5 μm, which is approximately one-forth of the maximum depth in the Y direction.
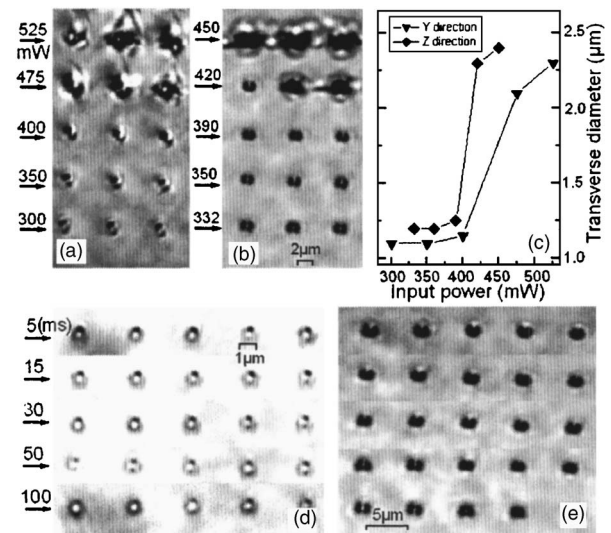
Now let us turn to the effect of the input power on the transverse size of the voids. As shown in Fig. 3(a), the transverse diameters of the voids in the Y direction at a given depth of 30 μm are almost unchanged (about 1.1 μm) when the input power is from 300 to 400 mW. At a higher power of 475 and 525 mW, the size of the voids increases dramatically to approximately 2.2 μm. But the surfaces of the voids seem not smooth and some cracks near the voids can be observed because the stress surrounding the voids produced by such high power exceeds the endurance of the crystal. In the Z direction, similar phenomena are observed for a given depth of 10 μm, as shown in Fig. 3(b). The diameter of the void is approximately 1.25 μm with the power from 332 to 390 mW. Further increase the power to 420 mW, the diameter of the void jumps to 2.2 μm. The most left void at the power of 420 mW is much smaller than other voids at this power but very similar to the voids at a lower power. This feature indicates that 420 mW is a threshold to generate large void with a diameter of 2.3 μm. The transverse diameters as a function of the input power in the Y and Z direction are plotted out in Fig. 3(c). Figures 2(e) and 3(c) indicate that as long as the threshold condition is satisfied, one can fabricate the voids that exhibit well-confined size in both axial and transverse directions.

Unlike the microexplosion process in the polymers,[10] there is no obvious change in the size of the voids for the exposure time between 5 ms (the minimum response limit of the shutter) and 100 ms in both the Y and Z directions of the $LiNbO_3$ crystal, as shown in Figs. 3(d) and 3(e). A possible reason is that the void is generated by the first one or several pulses. The following pulses are scattered by the void and therefore do not contribute to the volume of the void.
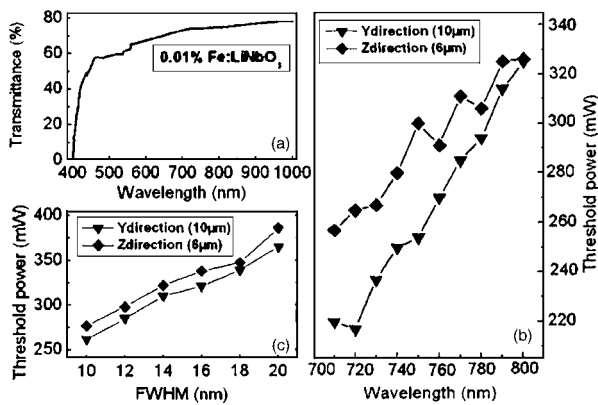
FIG. 4. (a) Transmission spectra of a 2-mm-thick Fe:LiNbO$_3$ crystal; (b) the wavelength response and (c) spectra distribution response of the microexplosion in the Y and Z directions.

The LiNbO$_3$ crystal is transparent in the region from 0.45 to 5 μm. Figure 4(a) shows the transmission spectra of a 2-mm-thick Y-cut LiNbO$_3$ crystal in the visible and near infrared region. One can see that the transmittance drops sharply at the wavelength shorter than 0.45 μm and there is no obvious linear absorption at wavelength 780 nm with which the voids are generated. Therefore, it is expected that the microexplossion process with laser irradiation of 780 nm should be a two-photon absorption process. To confirm this point, we studied the wavelength response of the LiNbO$_3$ crystal for the generation of voids. Figure 4(b) shows the threshold power as a function of wavelengths at a depth of 10 μm in the Y direction and at a depth of 6 μm in the Z direction. The spectral width of the laser irradiation is set to approximately 15 nm in full width at half maximum (FWHM), which corresponds to a pulse width of 45–50 fs for wavelengths of 720–800 nm. One can see that microexplosions can occur in a large wavelength range from 720 to 800 nm, which is approximately twice of the linear (one-photon) absorption range. The increasing of the threshold power with the wavelength suggests that the two-photon absorption efficiency is lower at longer wavelengths in the wavelength range of 720–800 nm.

Figures 2–4 imply that the fabrication depth in the Y direction is larger than that in the Z direction. This feature is caused by the anisotropy of the refractive indices in these two directions. It is well known that when a light beam impinges on a uniaxial crystal, it splits into ordinary rays (o rays) and extraordinary rays (e rays). The refractive index of o rays, n_o, is independent of the propagation directions, while the refractive index of e rays changes from n_o along the optic axis direction to n_e in the direction perpendicular the optic axis. LiNbO$_3$ is a negative uniaxial crystal with n_o of 2.26 and n_e of 2.18 at the wavelength of 780 nm.[19] For the NA 1.4 objective used in the present work, the maximum angle of incidence in the crystal is approximately 39.5°. The geometrical average of the refractive indices over the angle of incidence is 2.19 and 2.25 when the laser beam is focused along the Y and Z directions, respectively.

On the other hand, spherical aberration can happen when a laser beam is focused through the interface between two media of mismatched refractive indices.[17] Such spherical aberration leads to the distortion of the focal spot and the reduction of the intensity the focus. The larger the difference of the refractive indices, the stronger the reduction.[18] Therefore,

the larger average refractive index in the Z direction results in stronger spherical aberration than in the Y direction, which consequently reduces the maximum fabrication depth in generation of voids in the Z direction, as shown in Fig. 2.

The effect of the anisotropy of the LiNbO$_3$ crystal on the threshold power is also evidenced from the threshold powers at 790 nm with different spectral FWHMs in the Y and Z directions, as shown in Fig. 4(c). The threshold powers in the Y direction at a depth of 10 μm are even lower than those in the Z direction at a depth of 6 μm. It can also be seen that the threshold power increases as the FWHM increases. The main reason is a chromatic aberration caused by the spectral distribution of the laser light because the rays of different wavelengths are focused at different positions in the crystal. A larger FWHM results in a stronger chromatic aberration effect and therefore a lower peak power at a given energy.

In conclusion, microvoids can be generated in the high refractive index Fe:LiNbO$_3$ crystal by using a femtosecond laser-induced microexplosion method based on two-photon excitation. Quasispherical microvoids can be generated using the near threshold power depending on the fabrication depth. Due to the anisotropic property of the crystal, the effect of spherical aberration caused by the refractive index mismatch and chromatic aberration resulting from the finite spectral width of the laser in the Y direction is weaker than that in the Z direction. Accordingly, the maximum fabrication depth in the Y direction is approximately four times as large as than that in the Z direction. The maximum fabrication depth of 115 μm in the Y direction indicates that this technique has potential applications for fabricating 3D microstructures.

[1]D. Du, X. Liu, G. Korn, J. Squier, and G. Mourou, Appl. Phys. Lett. **64**, 3071 (1994).
[2]D. v. d. Linde and H. Schuler, J. Opt. Soc. Am. B **13**, 216 (1996).
[3]B. C. Stuart, M. D. Feit, S. Herman, A. M. Rubenchik, B. W. Shore, and M. D. Perry, J. Opt. Soc. Am. B **13**, 459 (1996).
[4]E. N. Glezer, M. Jilosavljevic, L. Huang, R. J. Finlay, T.-H. Her, J. P. Callan, and E. Mazur, Opt. Lett. **24**, 2023 (1996).
[5]C. B. Schaffer, E. N. Glezer, N. Nishimura, and E. Mazur, Proc. SPIE **3269**, 36 (1998).
[6]E. N. Glezer and E. Mazur, Appl. Phys. Lett. **71**, 882 (1997).
[7]D. Day and M. Gu, Appl. Phys. Lett. **80**, 2404 (2002).
[8]H.-B. Sun, Y. Xu, K. Sun, S. Juodkazis, M. Watanabe, S. Matsuo, H. Misawa, and J. Nishii, Proc. Mater. Res. Soc. **605**, 85 (2000).
[9]M. J. Ventura, M. Straub, and M. Gu, Appl. Phys. Lett. **82**, 1649 (2003).
[10]G. Zhou, M. J. Ventura, M. R. Vanner, and M. Gu, Opt. Lett. **29**, 2240 (2004).
[11]G. Zhou, M. J. Ventura, M. Straub, and M. Gu, Appl. Phys. Lett. **84**, 4415 (2004).
[12]G. Zhou, M. J. Ventura, M. R. Vanner, and M. Gu, Appl. Phys. Lett. **86**, 011108 (2005).
[13]H.-B. Sun, Y. Xu, S. Juodkazis, K. Sun, M. Watanabe, S. Matsuo, H. Misawa, and J. Nishii, Opt. Lett. **26**, 325 (2001).
[14]H.-B. Sun, Y. Xu, S. Matsuo, and H. Misawa, Opt. Rev. **6**, 396 (1999).
[15]S. Saltiel and Yu. S. Kivshar, Opt. Lett. **25**, 1204 (2000).
[16]S. Mingaleev and Y. Kivshar, Opt. Photonics News **13**, 48 (2002).
[17]Min Gu, *Advanced Optical Imaging Theory* (Springer, Berlin, 2000).
[18]D. Day and M. Gu, Appl. Opt. **37**, 6299 (1998).
[19]G. J. Edwards and M. Lawrence, Opt. Quantum Electron. **16**, 373 (1984).